

The Optoelectronic Properties of PbS Nanowire Field-Effect Transistors

Seunghyun Lee, Jin-Seo Noh, Jeongmin Kim, MinGin Kim, So Young Jang, Jeunghee Park, and Wooyoung Lee

Abstract—We report on the optoelectronic properties of individual PbS nanowires prepared by gas-phase substitution reaction of pre-grown CdS nanowires. The PbS nanowires synthesized by this method were found to be single crystals with high quality. A combination of electron-beam lithography and a lift-off process was utilized to fabricate individual 62-nm-thick PbS nanowire field-effect transistors (FETs). The nanowire FETs showed pronounced photoconductivity under light illumination while they were highly resistive in the dark environment. The conductivity increased by more than 40 folds in the presence of light. Our results are the first demonstration of the highly efficient photoresponse of individual single-crystalline PbS nanowires and provide insights into future works on nanostructured PbS optoelectronics.

Index Terms—Field-effect transistor (FET), PbS nanowires, photoconductivity.

I. INTRODUCTION

L EAD sulfide (PbS) is an intriguing IV–VI semiconductor with a narrow band gap of 0.41 eV and large Bohr radius of 18 nm in its bulk state [1], making it an attractive candidate for potential applications in optoelectronic fields such as solar cells and infrared detectors. Especially, PbS nanosturctures are promising materials which can be applied in various fields, such as infrared emission and detection, biological imaging, photovoltaics, and solar cells [2]–[6]. This material is also known to exhibit strong size effects, leading to quantum confinement and semiconductor-to-metal transition in various nanostructures [7]. For instance, it has been reported that the bandgap of PbS nanowire exceeds 1 eV when its diameter shrinks below 3 nm [8], and a 30 nm PbS nanowire undergoes a blue shift compared to 60 nm nanowire in their absorption spectra [9]. In

addition, PbS has been considered for thermoelectric applications because its thermoelectric figure-of-merit ZT is relatively high (0.8 at 723 K) in bulk [10]. PbS nanostructures, particularly, PbS nanowires are of critical importance for improved performance in these areas as well, due to enhanced surface phonon scattering and quantum confinement effect of conduction electrons in the nanostructures. Despite the potentials of the PbS nanowires for use in such broad fields, their properties, especially, electrical or optoelectronic properties have not been investigated enough. Parts of the reasons are attributed to difficulties in growing single-crystalline PbS nanowires and fabricating devices on individual nanowires.

In this study, we present the optoelectronic properties of field-effect transistors (FETs) elaborately fabricated on individual single-crystalline PbS nanowires. The PbS nanowires are synthesized by gas-phase substitution reaction of pre-grown CdS nanowires. We briefly introduce the nanowire growth technique because details have already been reported elsewhere [11].

II. EXPERIMENTAL PROCEDURES

Single-crystalline rock-salt PbS nanowires were synthesized using the gas-phase substitution reaction of pre-grown CdS nanowires. For the chemical conversion of CdS nanowires into PbS nanowires this ultimate cation-exchange process, we synthesized CdS nanowires at the very beginning. The CdS nanowires were grown using the chemical vapor transport (CVD) method, in which the CdS (99.98%, Aldrich) powder was placed in a quartz boat loaded inside a quartz tube reactor. A silicon substrate coated with Au catalyst was positioned at a distance of 10 cm from the quartz boat. As the source was evaporated at 850 °C for 1 h under argon flow (300 sccm), high-density CdS nanowires were grown on the substrates at about 700 °C. Then, the pre-grown CdS nanowires were placed in the reactor and PbCl₂ powders were evaporated for 10–60 min at temperatures of 600 °C. The identity and crystallinity of nanowires thus synthesized were analyzed by means of transmission electron microscopy (TEM) and electron diffraction.

For the fabrication of a FET on individual nanowires, the PbS nanowires were dispersed by applying a drop of isopropyl alcohol (IPA) containing free-standing nanowires onto a Si (100) substrate with a thermal oxide layer [12]. The Si substrate was highly doped to be used as a back gate. In this study, small-sized nanowires, particularly, 62-nm-diameter nanowires were on focus to take the advantage of the bandgap enlargement effect of PbS at the very thin nanowires. A combination of electron-beam lithography and a lift-off process was utilized to fabricate individual nanowire devices. For reliable electrical ohmic contacts, a plasma etching technique was employed to

Manuscript received August 2, 2012; accepted August 19, 2013. Date of publication September 5, 2013; date of current version November 6, 2013. This work was supported in part by the Priority Research Centers Program (2009-0093823), in part by the Pioneer Research Center Program (2013008070), and in part by the Converging Research Center Program (2012K001321) through the National Research Foundation of Korea (NRF) funded by the Ministry of Education, Science and Technology. J. Park acknowledges support from NRF (2011-001-5235). The review of this paper was arranged by Associate Editor Y.-H. Cho.

S. Lee, J. Kim, M. Kim, and W. Lee are with the Department of Materials Science and Engineering, Yonsei University, Seoul 120-749, Korea (e-mail: sebin0524@hanmail.net; jmkim@yonsei.ac.kr; hellengford@yonsei.ac.kr; wooyoung@yonsei.ac.kr).

J.-S. Noh is with the Department of Nano-Physics, Gachon University, Seongnam 461-701, Korea (e-mail: jinseonoh@gachon.ac.kr).

S. Y. Jang and J. Park are with the Department of Chemistry, Korea University, Joachiwon, Chungnam 339-700, Korea (e-mail: ckrgkthdud@naver.com; parkjh@korea.ac.kr).

Color versions of one or more of the figures in this paper are available online at <http://ieeexplore.ieee.org>.

Digital Object Identifier 10.1109/TNANO.2013.2280911

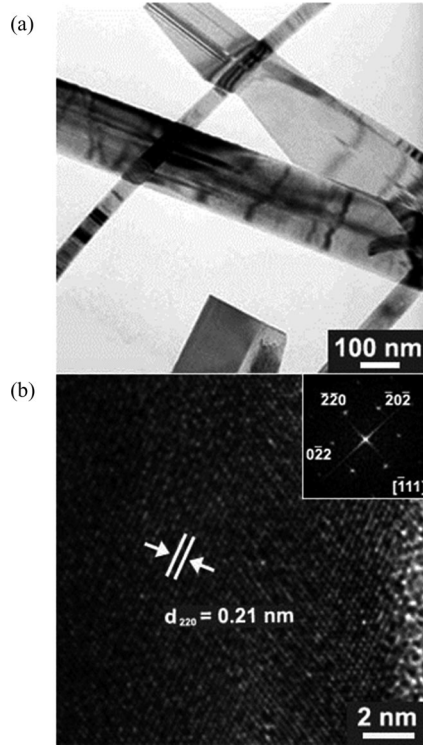


Fig. 1. (a) TEM image of PbS Nanowires synthesized by gas-phase substitution technique. (b) Lattice-resolved TEM image of a PbS nanowire. The distance between the (220) planes is about 0.21 nm. The corresponding SAED pattern, measured on the [1 1 1] zone axis, confirmed that the single-crystalline nanowires grew in the [1 1 0] direction (inset).

remove an oxide layer that forms on the outer surface of the nanowire, and Cr (5 nm)/Au (195 nm) electrodes were deposited *in situ* by sputtering.

III. RESULTS AND DISCUSSION

Fig. 1(a) shows a TEM image of the PbS nanowires grown by gas-phase substitution reaction of pre-grown CdS nanowires. The PbS nanowires were found to grow to several hundred micrometers in length and span over a few tens to a few hundred nanometers in diameter. Fig. 1(b) exhibits the lattice-resolved TEM image of a PbS nanowire, demonstrating its single-crystalline structure. The (220) fringes were found to be separated by a distance of 0.21 nm, which is equal to that of cubic PbS crystal ($a = 5.94 \text{ \AA}$; JCPDS card no. 78-1058). The corresponding selected-area electron diffraction (SAED) pattern, measured on the [1 1 1] zone axis, confirmed that the single-crystalline nanowires grew in the [1 1 0] direction (inset). Our previous work gives a detailed analysis of the elemental structure of the synthesized PbS nanowires using gas-phase substitution reaction at 600 °C, in which the growth direction was determined to be [1 1 0], and has an equal lattice parameter with the cubic PbS crystal [11].

Fig. 2(a) shows our four-probe device fabricated on an individual PbS nanowire with 62 nm. The four-probe measurement technique was used to remove the additional source of resistance, such as contact resistance. The current source was

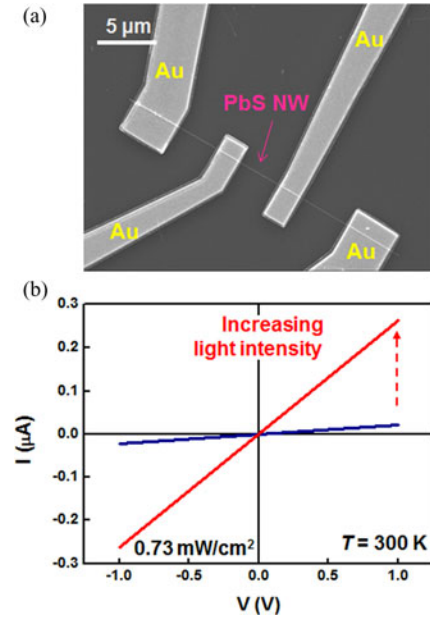


Fig. 2. (a) SEM image of a four-probe device fabricated on an individual PbS nanowire. (b) Current (I) versus voltage (V) curves of the nanowire device with varying light intensity at room temperature.

connected to the two electrodes on the edge and the voltage was measured using the two centered electrodes. The technique prevents voltage drop due to contact junction by dividing the current path from the voltage measuring circuit. The light-dependent current versus bias voltage (I - V) characteristics were analyzed on this device using a Keithley 236 Source-Measure Unit and 2182 nano-voltmeter.

Optoelectronic measurements were performed using MR16 halogen lamp source and TES 1335 light meter equipped to a probe station. To determine the optoelectronic transport in visible light, an optical wavelength filter which is transparent between 420 and 680 nm was used. The lamplight was focused on the device, and the half maximum of the spectrum from the lamp is from 540 to 665 nm. The light intensity was swept from 0 to 15 mW/cm². The I - V characteristics were measured at each light intensity. In the dark, the nanowire device is quite resistive [blue line, Fig. 2(b)] with typical current levels being a few nanoampere to a few volts of applied bias. Such a high resistance can be attributed to the fact that the nanowires were basically undoped; thus, any carriers should be generated either from thermal excitation or from a low density of unintentional dopant atoms incorporated during the growth process. Furthermore, metal contacts were not annealed in order to avoid metal diffusion into the channel, which probably increased contact resistance at each metal–nanowire contact. The high initial resistance of the nanowire device also rules out the probability that a significant number of surface states are electrically activated. From these points, it is reasonable to infer that any substantial change in transport of the nanowire device is caused by a change in electrical properties of the nanowire itself. To examine the optical response of the PbS nanowire device, transport measurements were performed under lamplight with its intensity varied over 0 and 15 mW/cm². The resistance

of the nanowire device is found to substantially decrease with increasing light intensity due to the pronounced photoconductivity [red line, Fig. 2(b)]. As aforementioned, this drastic change in transport arose from a fundamental change in the nanowire properties and a significant increase in carrier population, which results from electron–hole pair generation driven by absorbed light, is responsible for that. As a support for this, the increase in current was nearly symmetrical at both positive and negative biases for all devices, irrespective of ohmic or rectifying, which indicates that equal numbers of electrons and holes were generated during light illumination. Note that PbS is a direct bandgap semiconductor ($E_g = 0.41$ eV, λ cutoff = 3.0 μm) and is expected to show strong photoconduction at relatively large wavelengths [13].

To further investigate the optoelectronic properties and majority carrier type of PbS nanowires, FETs were fabricated and measured on individual nanowires. Back-gate FET structures were used with a thick oxide (500 nm) on Si back-gate, as illustrated in Fig. 3(a). Typical gate-dependent source-to-drain current ISD-VSD curves recorded on an individual PbS nanowire are shown in Fig. 3(b). The I - V data obtained from zero gate voltage ($V_G = 0$ V), which account for contributions from multiple parts such as PbS channel, contacts, and surface oxide, yield a resistivity of $3.9 \times 10^2 \Omega\cdot\text{cm}$ that is slightly higher than that of conventional semiconductors. When V_G is tuned to be increasingly negative (positive), the conductance (G) increases (decreases). This gate dependence indicates that the PbS nanowire is a p-type semiconductor. However, the modulation of the drain current by the gate voltage is very weak. Although there is no clear evidence to explain this phenomenon, it is thought that the dielectric layer (SiO_2 , $t = 500$ nm) is too thick to inject carriers into PbS nanowire using the field effect. Furthermore, the PbS nanowire has an oxide layer on its surface resulting in decrease of the effect. Similar I - V trends depending on V_G were observed under lamp light, confirming that the majority carrier type does not change. Surprisingly, the conductance of the FET strongly depends on the intensity of illuminating light and it drastically increases with increasing the light intensity at zero gate bias ($V_G = 0$ V), as shown in Fig. 3(c). This is analogous to the behavior observed in four-probe devices, which was previously discussed, and represents that a carrier population generated by light absorption is dominant in transport in the absence of gate bias. One interesting point with Fig. 3(c) is that the current does not increase linearly with light intensity, reflecting that carriers generated in excess of an equilibrium population are recombined to keep a stable carrier concentration [4].

The relative impacts of gate biasing and light illumination on transport properties would become clearer if transport is measured with sweeping gate biases under lamp light with a fixed intensity. Fig. 4(a) shows source-to-drain conductance versus gate bias (GSD-VG) curves measured with and without light illumination. The light intensity of 0.73 and 10.3 mW/cm^2 was selected, and the data in the dark were obtained as a control for comparison. For all cases, GSD does not change significantly with sweeping the gate bias within $V_G = \pm 60$ V, reflecting that carrier injection from source activated by barrier lowering

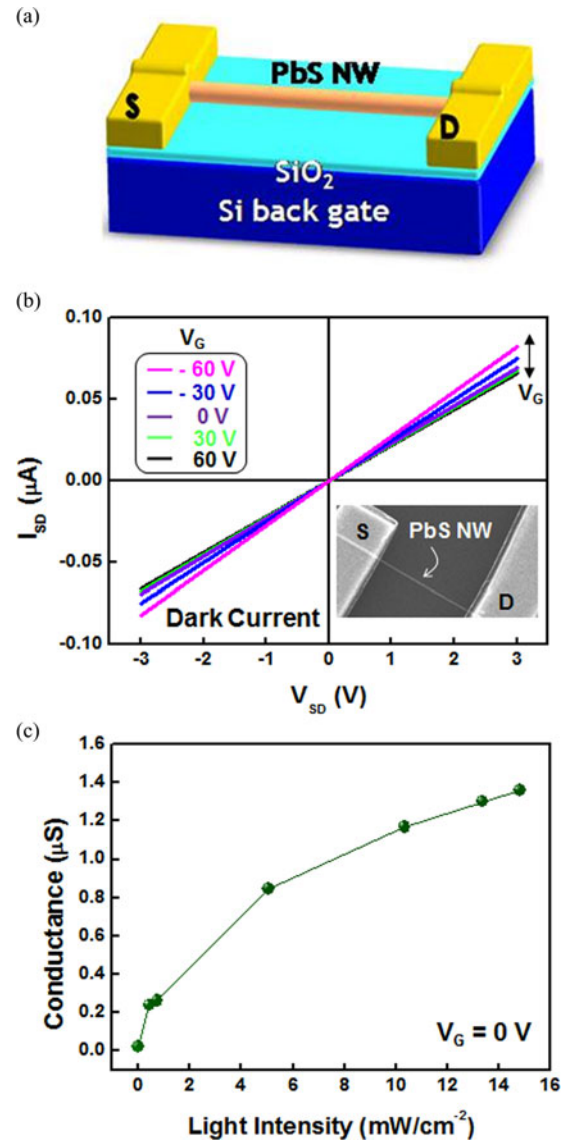


Fig. 3. (a) Schematic of a FET fabricated on an individual PbS nanowire. (b) ISD-VSD curves recorded on a 62-nm-diameter PbS nanowire at varying gate biases (V_G). The respective colors correspond to $V_G = -60$, -30 , 0 , 30 , and 60 V, respectively. (Inset) an SEM image of a PbS nanowire FET. (c) Conductance of the FET versus light intensity measured without a gate bias at 300 K.

between the source and channel is not enough to sizably change the conductance. In contrast, the GSD jumps up by more than 40 folds in the presence of light with respect to the dark current at each gate bias. These results suggest that optically generated carriers play a dominant role in transport of PbS nanowire FETs with a minor effect of gate modulation. This aspect is also supported by the comparison of ISD–VSD curves that were obtained from largely different gate biases (-60 and 60 V) under lamp light with an identical intensity ($10.3 \text{ mW}/\text{cm}^2$). It is found from Fig. 4(b) that the three ISD–VSD curves are nearly overlapped, underscoring that carriers injected from source have no meaningful effects on the overall transport behavior under the condition of light illumination with a moderate intensity. The

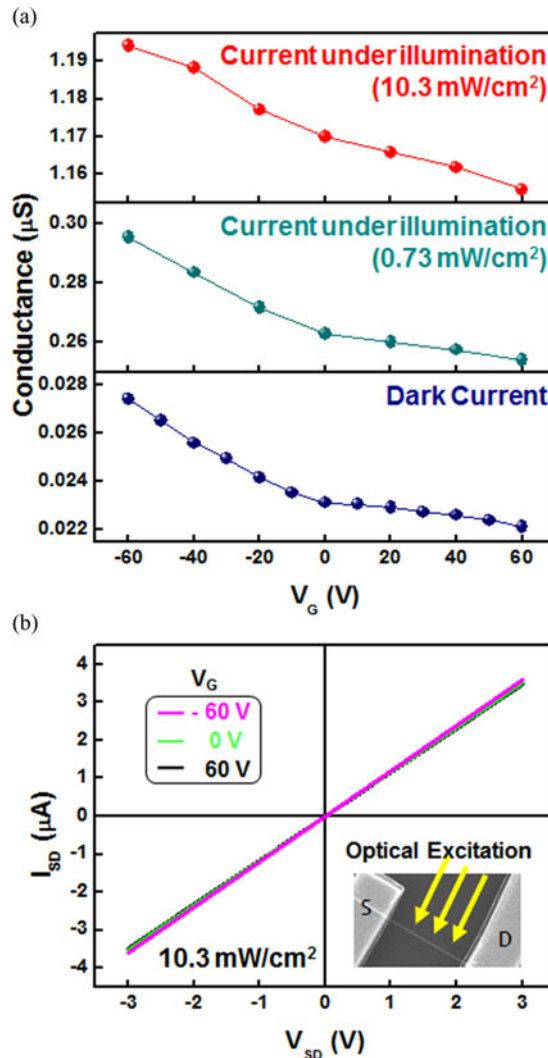


Fig. 4. (a) GSD-VG curves of an individual PbS nanowire FET measured without and with light illumination (10.3 mW/cm^2) at room temperature. (b) Comparison of ISD-VSD curves measured at three different gate biases ($V_G = -60, 0, \text{ and } 60 \text{ V}$) under lamp light with an intensity of 10.3 mW/cm^2 .

strong optical response of our individual PbS nanowire devices relies on the highly single-crystalline nature of our nanowires and their high surface-to-volume ratio.

IV. CONCLUSION

In summary, high-quality, single-crystalline PbS nanowires with diameters of 60–120 nm were synthesized by gas-phase substitution reaction of pre-grown CdS nanowires. The resistance of four-probe device fabricated on these nanowires was drastically reduced under lamp light illumination due to pronounced photoconduction. Back-gated field-effect transistors were fabricated on individual PbS nanowires and their optoelectronic properties were characterized. The PbS nanowire FETs behaved to be slightly p-doped, due primarily to unintentional

doping during nanowire growth. The FETs were resistive without a gate bias and their conductance was not significantly modulated by gate biasing between $\pm 60 \text{ V}$. On the other hand, the conductance substantially leapt by more than 40 folds under light illumination, regardless of the existence of gate bias. This indicates that charge carriers generated by light absorption dominate transport properties of PbS nanowires. The strong optical response of PbS nanowires coupled with their simple growth technique holds much promise for applications in future optoelectronics and optical devices.

REFERENCES

- [1] F. W. Wise, "Lead salt quantum dots: the limit of strong quantum confinement," *Acc. Chem. Res.*, vol. 33, pp. 773–780, 2000.
- [2] L. Bakueva, S. Musikhin, M. A. Hines, T. W. F. Chang, M. Tzolov, G. D. Scholes, and E. H. Sargent, "Size-tunable infrared (1000–1600 nm) electroluminescence from PbS quantum-dot nanocrystals in a semiconducting polymer," *Appl. Phys. Lett.*, vol. 82, pp. 2895–2897, 2003.
- [3] L. Bakueva, I. Gorelikov, S. Musikhin, X. S. Zhao, E. H. Sargent, and E. Kumacheva, "PbS quantum dots with stable efficient luminescence in the near-IR spectral range," *Adv. Mater.*, vol. 16, pp. 926–929, 2004.
- [4] S. A. McDonald, G. Konstantatos, S. G. Zhang, P. W. Cyr, E. J. D. Klem, L. Levina, and E. H. Sargent, "Solution-processed PbS quantum dot infrared photodetectors and photovoltaics," *Nat. Mater.*, vol. 4, pp. 138–142, 2005.
- [5] A. J. Nozik, "Exciton multiplication and relaxation dynamics in quantum dots: Applications to ultrahigh-efficiency solar photon conversion," *Inorg. Chem.*, vol. 44, pp. 6893–6899, 2005.
- [6] T. Rauch, M. Böberl, S. F. Tedde, J. Fürst, M. V. Kovalenko, G. Hesser, U. Lemmer, W. Heiss, and O. Hayden, "Near-infrared imaging with quantum-dot-sensitized organic photodiodes," *Nat. Photon.*, vol. 3, pp. 332–336, 2009.
- [7] A. K. Dutta, T. Ho, L. Zhang, and P. Stroeven, "Nucleation and growth of lead sulfide nano- and microcrystallites in supramolecular polymer assemblies," *Chem. Mater.*, vol. 12, pp. 1042–1048, 2000.
- [8] S. Mandal and R. Pati, "Quantum confinement and phase transition in PbS nanowire: A first principles study," *Chem. Phys. Lett.*, vol. 479, pp. 244–247, 2009.
- [9] C. Wu, J. B. Shi, C. J. Chen, Y. C. Chen, P. F. Wu, and J. Y. Lin, "Correlation between structural and optical properties of 30 nm and 60 nm lead sulfide nanowires," *Mater. Lett.*, vol. 61, pp. 4659–4661, 2007.
- [10] M. Fardy, A. I. Hochbaum, J. Goldberger, M. M. Zhang, and P. Yang, "Synthesis and thermoelectric characterization of lead chalcogenide nanowires," *Adv. Mater.*, vol. 19, pp. 3047–3051, 2007.
- [11] S. Jang, Y. Song, H. Kim, Y. Cho, Y. Seo, G. Jung, C. Lee, J. Park, M. Jung, J. Kim, B. Kim, J. Kim, and Y. Kim, "Three synthetic routes to single-crystalline PbS nanowires with controlled growth direction and their electrical transport properties," *ACS Nano*, vol. 4, pp. 2391–2401, 2010.
- [12] S. Lee, W. Shim, S. Jang, J. Roh, P. Kim, J. Park, and W. Lee, "Thermoelectric properties of individual single-crystalline PbTe nanowires grown by a vapor transport method, thermoelectric properties of individual single-crystalline PbTe nanowires grown by a vapor transport method," *Nanotechnology*, vol. 22, pp. 295707-1–295707-6, 2011.
- [13] H. Zogg, S. Blunier, T. Hoshino, C. Maissen, J. Masek, and A. N. Tiwari, "Infrared sensor arrays with 3–12 μm cutoff wavelengths in heteroepitaxial narrow-gap semiconductors on Si substrates," *IEEE Trans. Electron Devices*, vol. 38, pp. 1110–1117, 1991.